Sustainable Energy Research

REVIEW

Open Access

Selection process of photovoltaic standalone pumping systems

Fathy A. Syam[1*] and Osama M. Arafa[1]

Abstract

The application of a standalone photovoltaic (PV) system for water pumping has increased nowadays in remote areas of developing countries due to proven economic feasibility compared to other traditional alternatives. Pump–motor set manufacturers always give the pump characteristic at the motor's nominal speed. The traditional selection process of pumps depends simply on selecting a pump with the highest peak efficiency that can satisfy the desired duty point with its peak efficiency occurring at that duty point. However, this simple selection process could lead to selecting a pump that is not the best selection from among a given set of candidate pumps for the targeted service.

In this paper, this fact is revealed by comparing two pumps each having the same peak efficiency and each of them can operate at the desired duty point with one critical difference between the two pumps. One of the two pumps has its peak efficiency occurring at the right of the duty point and the other has its peak efficiency occurring at the left of the desired duty point. The methodology of this research is based on calculating the daily efficiency of each pump by calculating the hydraulic power produced with the electrical power of the solar system. The efficiency calculation has been calculated over two working days, one with low radiation (3 kW/m^2/day) and the other with high radiation (7.3 kW/m^2/day). The search for the all-day efficiency for low radiation levels revealed that the pump with left-shifted peak efficiency gives 42.5% while for high radiation level gives 40.3%. In two cases the pump with left-shifted peak efficiency constitutes the best choice.

Highlights

- We propose a new method to select the best PV pumping system.
- The proposed method uses a simplified method to compare between two completely identical PV pumping systems except for the use of two different centrifugal pumps.
- This method aims at selecting the proper centrifugal pump according to maximum all-day efficiency.
- The proposed method was tested under the different solar radiation levels.

Keywords Solar Energy, PV system, Pump System, Centrifugal Pump, Duty Point, Induction Motor, Pump Efficiency

*Correspondence:
Fathy A. Syam
fathy@eri.sci.eg
[1] Researcher at Power Electronics & Energy Conversion Department, Electronics Research Institute, Cairo, Egypt

Introduction

Water pumping in many countries relies mainly on conventional electricity or diesel-generated electricity. It has become necessary to depend on a solar water pumping system to reduce the use of diesel fuel or coal-based electricity. The use of diesel water pumping systems leads to noise and air pollution in addition to the exorbitant cost of fuel. The photovoltaic industry has seen significant advances in both improving efficiency and reducing costs in the past two decades. The initial total cost, operation and maintenance costs, and replacement of a diesel pump are 2 to 4 times higher than that of a PV pump. (Xie et al., 2021) compared the cost-effectiveness of solar PV and diesel energy for groundwater pumping for irrigation. The observed cost-effectiveness of solar-powered groundwater irrigation relative to diesel-powered groundwater irrigation varies across scenarios. Overall, the results of the study show that solar PV is a promising energy solution to support groundwater-fed irrigation development. In many cases, solar energy can serve as a substitute for diesel to power groundwater pumping for irrigation more economically and non-polluting to the environment.

(Chandel et al., 2015) found that the application of standalone direct-coupled electromechanical PV systems for water pumping has gained wide popularity in remote areas of developing countries recently. Providing water for agricultural and domestic use using photovoltaic water pumping technology is a sustainable and environmentally friendly solution. Solar water pumping system is known to be more reliable and more effective for irrigation applications especially in remote areas compared to other alternative systems. (Kolhe et al., 2004) analyzed the performance analysis of the directly PV-powered permanent magnet motor coupled with a centrifugal pump at different solar intensities and corresponding cell temperatures. It has been observed that the system operates most of the daytime because of its torque sufficiency even at low solar intensities.

(Allouhi et al., 2019) investigated the optimal configuration of a photovoltaic system supplying a submersible pump to meet the domestic water of five isolated houses located in a remote area. It has been ruled that the configuration with a maximum power point tracking (MPPT) converter is the most convenient method to supply water needed by the five dwellings considered in the case study. The variations in the performance ratio indicate that the MPPT configuration is higher than that of the direct coupling system in general. Moreover, the missed water ratio for the MPPT configuration was found less than the direct coupling one.

(Renu et al., 2017) analyzed the effect of radiation and temperature changes on the amount of water produced by photovoltaic water pumps. A methodology is proposed to optimize the performance of PV pumps based on water head and pump duty point using the most common site conditions. The selection of optimum array sizing for a pump has been done based on the occurrence of desirable input power and subsystem efficiency. (Boutelhig et al., 2011) investigated two different PV pumping system configurations based on two different submersible pump performances. The selection of a suitable PV pumping system may be based on the daily required volume of water and the overall system efficiency and cost.

(Abdelmalek et al., 2011) carried out an experimental study to investigate the performance of a simple, directly coupled photovoltaic-powered water pumping system. The system comprises a PV array, a Direct Current (DC) motor, and a centrifugal pump. The experiment was conducted over a period of 4 months and the system performance was monitored under different climatic conditions and varying solar radiation with two static head configurations. It has been observed that the system is more suitable for low delivery flow rate applications. The efficiency of the system can increased by carefully selecting the size of the PV array, its orientation, and the motor–pump system.

(Ghoneim, 2006) presented the performance optimization of a photovoltaic-powered water pumping system in the Kuwait climate. The direct-coupled photovoltaic water pumping system studied consists of the PV array, centrifugal pump, DC motor, a storage tank that serves a similar purpose to battery storage, and a maximum power point tracker to improve the energy consumption rate of the system. A computer simulation program is developed to determine the performance of the proposed system in the Kuwait climate. The simulation program consists of a model for the PV array with a maximum power point tracker and models for both the DC motor and the centrifugal pump. The size of the PV array, PV array orientation, and the pump–motor–hydraulic system characteristics are varied to achieve the optimum performance for the proposed system.

(Chandrasekaran et al., 2012) achieved the simulation of a PV array-based DC motor pumping system and permanent magnet motor pumping system. The comparison of the two systems has been done and proved a simple but efficient photovoltaic water pumping system among them. Motors and centrifugal pumps operate at variable speeds in a photovoltaic pumping system. However, the characteristics of motors and pumps are usually only given for a single voltage and speed. To analyze the operation of a pumping system, where solar radiation causes variation in the photovoltaic power, the input/output relationship of the motor pump assembly and motor characteristics must be determined. The results obtained from the simulation of the system are satisfactory. It is found that a permanent magnet motor pumping system is better.

(Abdourraziq and Bachtiri, 2017) carried out a comparative study on two similar PV pumping systems, one of them is driven by a permanent magnet DC motor, and the other is driven by an AC motor. The studied AC system consists of a PV array, a DC–DC boost converter, an inverter, a motor–pump set, and a storage tank. In addition, a maximum power point tracking algorithm is used to improve the energy consumption rate of the PV system. The comparison was carried out to define the characteristics and the performance of each system. Each subsystem is modeled to simulate the whole system. The results obtained from the simulation of the system are satisfactory and will make it possible to provide a very high speed of rotation in an AC motor compared to a Permanent Magnet (PM) motor, which is an important source of power for driving a pump.

(Gasque et al., 2020, 2021) analyzed a method for distributing the power generated in a photovoltaic pumping system equipped with two equal pumps, working in parallel. The system equipped with two pumps was investigated. Experimental tests at five different working frequencies, and at six pumping heads were carried out. The results for the different pumping heads show differences between higher and lower heads. (Gutierrez et al., 2021) evaluated the efficiency of a photovoltaic water pumping system. Hydraulic performance needs to be determined under the solar irradiance available. Performance ratio (PR) was used to determine the hydraulic performance of a photovoltaic pumping system, operated by a variable frequency inverter coupled to a conventional alternating current surface pump. (Almeida et al., 2018) evaluated a new method for selecting a pump for large-power PV irrigation systems working at a variable frequency. This can have a significant impact since the traditional way of selecting the pump is based on maximizing the efficiency of the pump at a single duty point (normally at the nominal operating frequency), which is not useful for PV irrigation systems working at variable frequencies. The proposed method starts by considering the pumps with *H*–*Q* curves with a high slope and the duty point in the right-hand third of the curve to ensure a wide range of operating frequencies. Then, the efficiency within the whole range of frequencies. Also, (Yadav et al., 2019) investigated of the energy efficiency of PV pumping systems based on solar radiation, temperature, and operational heads. The study identifies the shortcomings in the conventional design method based on the Best Efficiency Point (BEP) concept. According to this concept, a centrifugal pump has an optimum efficiency duty point, known as the Best Efficient Point (BEP), usually specified by the manufacturer. (Wanderley et al., 2021) confirmed that the assumption of the companionship of best hydraulic efficiency to the selection of a pump with the highest efficiency at the desired nominal duty point is valid only to fixed frequency and voltage type pumps. However, in the case of PV pumping systems, due to variations in the solar intensity, ambient temperature, and operational water heads, the BEP concept does not offer the best efficiency design.

Many studies have been done to evaluate the performance of the pumping system. (Odeh, 2013) investigated photovoltaic pumping systems for three years of field data analysis. (Belkacem, 2013) designed the pumping system based on two important elements: the PV array and the storage tank. (Babkir, 2018) developed a comparative assessment model for three types of solar water pumps based on the concept of levelized energy cost. (Koor et al., 2016; Roberto Valer et al., 2016) studied the operation of the pumping system to obtain the best efficiency with variable rotation speed.

It is interesting to know that a similar situation exists in electrical transformer design. Power and distribution transformers are differentiated on the basis of service type. Power transformers are supposed to operate at or near full load most of the time and therefore, their peak efficiency should be targeted by design as close as possible to a high-loading condition. While distribution transformers always operate at partial load and here stems the concept of all-day efficiency. Designers are therefore, requested to shift the peak efficiency occurrence to the left on the load axis to optimize the all-day efficiency. A similar concept is apparently applicable to PV pumping systems which operates at variable load most of the time.

This paper presents a comparison between two identical PV pumping systems, each of which supplies the same load at the same operating point (*H*, *Q*). The two pumps mainly have different *H*–*Q* curves, while having the same peak efficiency. This peak efficiency occurs at different values of flow rate for each pump. The research aims at selecting the proper centrifugal pump according to maximum all-day efficiency with different levels of solar radiation. This research provides great benefits to users in the field of agriculture and irrigation in remote places. Selecting the best pump saves the cost of daily operation.

The study is organized as follows: Section "Photovoltaic pumping system configuration (PVPS)" describes the PV system configuration covering the PV array, the motor, the centrifugal pumps, and the load hydraulic characteristics. Section "Methodology" describes the methodology of the system operation under given site conditions. Section "Selecting the proper pump" discusses the selection process of the proper pump. Section "Results and discussions" introduces the results and discussion. Section "Conclusion" includes the conclusion of this study.

Photovoltaic pumping system configuration (PVPS)

The configuration of the modeled PVPS is shown in Fig. 1. The system, which represents the most common configuration found in direct coupled PV pumping applications, is composed of a PV generator, a power control system

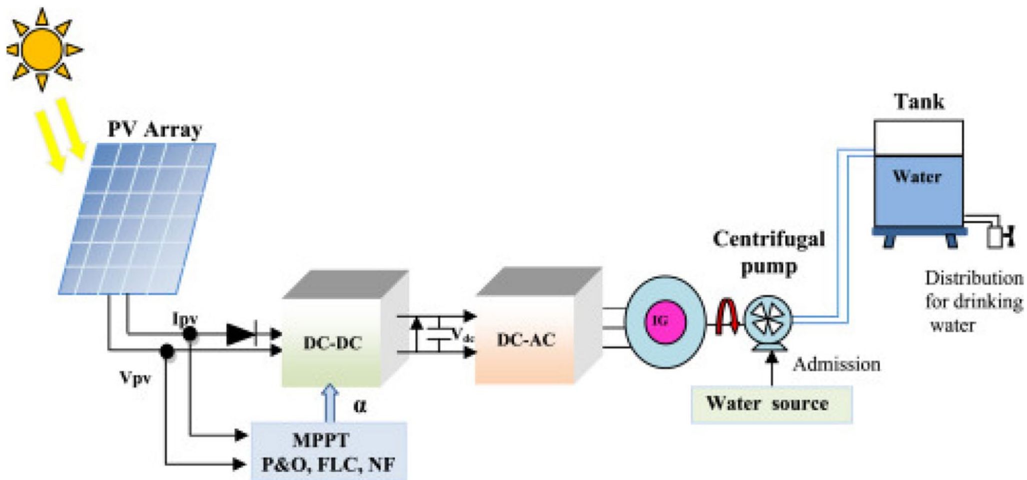

Fig. 1 Configuration of a direct-coupled PVPS

(Inverter and maximum power point tracking unit), an induction motor, and a centrifugal pump (Rahrah et al., 2015).

Methodology

Centrifugal pump characteristics

Both the *H*–*Q* curve and the efficiency versus flow rate curve (η_P-*Q*) characterize the performance of centrifugal pumps. The manufacturer's data sheet provides these curves at rated pump speed. However, in PVPS, the centrifugal pump operates at different speeds as the available solar resource varies. Such variable speed operation obeys the affinity laws that express the mathematical relationships between the several variables involved in pump performance. These variables include the pump's mechanical input power (Pm), the flow rate (*Q*), the water head (*H*), and the pump's rotating speed (*N*) (Alonso et al., 2003).

Figure 2 is adapted from a motor pump manufacturer company datasheet (SAER ELECTROPOMPE Software, 2019). It shows the *H*–*Q* and η_P–Q curves for the SAER ELECTROPOMPE Curvas-IR32-125A at rated speed. The best efficiency is given at $H=18.7$ m, $Q=16.4$ m^3/hr. At these conditions, the maximum efficiency is close to 56%.

Consider a pump rotating at speed N_1, at an operating point (H_1, Q_1). A new operating point for the pump (H_2, Q_2) can be reached by changing the pump speed to a new value N_2 given that (Bansal, 2010):

$$\frac{Q_1}{Q_2} = \frac{N_1}{N_2}\frac{D_1^3}{D_2^3} \tag{1}$$

$$\frac{H_1}{H_2} = \frac{N_1^2}{N_2^2}\frac{D_1^2}{D_2^2} \tag{2}$$

Substituting for $D1/D2$ from Eq. (1) into Eq. (2)

$$\frac{Q_1}{Q_2} = \frac{N_2^2}{N_1^2}\left(\frac{H_1}{H_2}\right)^{\frac{3}{2}} \tag{3}$$

For the same discharge flow rate ($Q_1 = Q_2$), the values of H_2 in terms of speed ratio and H_1 can be determined by rearranging Eq. (3) as follows:

$$H_2 = H_1\left(\frac{N_2}{N_1}\right)^{\frac{4}{3}} \tag{4}$$

Therefore, the *H*–*Q* curve for the specified pump at 2500 rpm (or any other arbitrary speed) can be determined given that the curve is known at 2900 rpm (rated pump speed) as shown in Fig. 3.

Characteristics curve of the hydraulic system

In a hydraulic system, the total head (*h*) against which the pump must operate is given by the sum of the static head, the drawdown of the water level, and the friction losses. Figure 4 illustrates the different water heads in a typical pumping application. The static head is 20.5 m and the friction factor (*k*) is about 5%. Equation (4) represents the system's *H*–*Q* curve, as given by several works in the literature (Ahonen et al., 2012).

$$H = h + kQ^2 \tag{5}$$

The required duty point for this system at $H=21.5$ m and $Q=12.8$ m^3/hr.

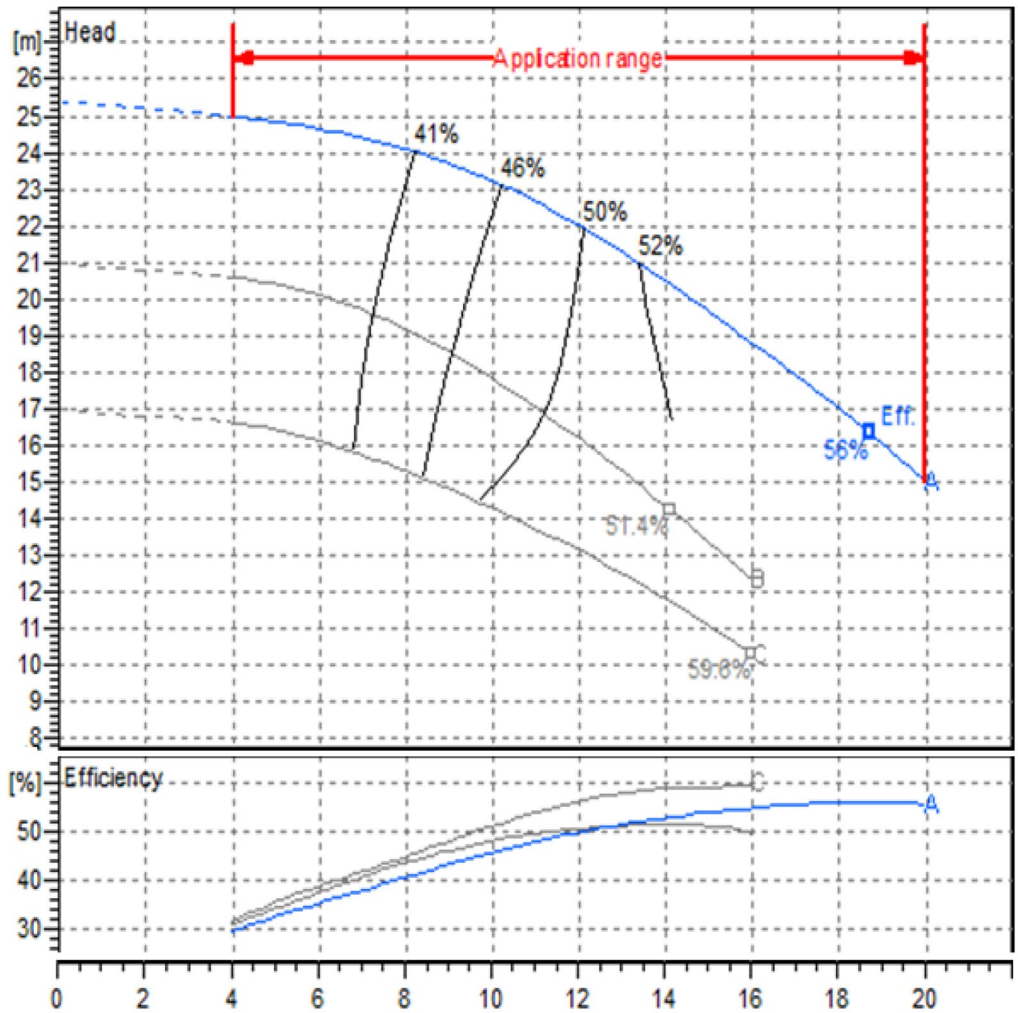

Fig. 2 Head and efficiency curve with flow rate (m^3/hr.)

Solar array

The size of the solar array used is determined by the rated power and efficiency of the motor. The pump used is powered by a motor that has 1.5 kW rated power and its efficiency at the rated power equals 0.82. The size of the solar array is determined according to the radiation values so that the maximum power produced by the array is approximately equal to the rated motor input power. The motor does not operate at a load greater than its rated load. The solar array area can be calculated from the following equation:

$$A = \frac{P_m}{\varnothing \eta_{pv} \eta_m \eta_c} \tag{6}$$

where,

A = Solar array area.
P_m = Motor rated output power.
$\varnothing$ = Maximum solar radiation.
η_{pv} = Efficiency of solar cell.
η_m = Efficiency of Electrical motor.
η_c = Efficiency of Power Control Unit.

The total number of modules can be calculated by dividing the total area by the area of one m1odule.

The solar module used is OPS-100M and its specifications are shown in Appendix.

Induction motor

A three-phase induction motor is used to drive the pump. The motor efficiency is important factor to calculate the input power of the pump and the output power from the solar array. The actual value of power during operation is variable due to radiation change. So, the motor is operating at partial load for some hours and motor speed is

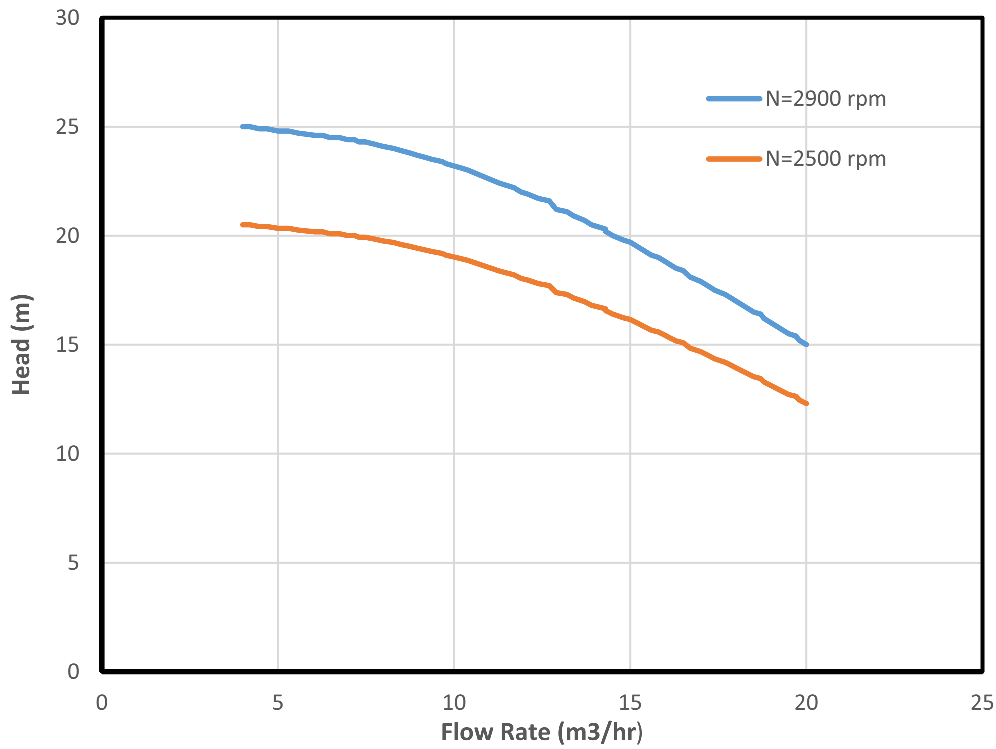

Fig. 3 The *H–Q* curve at different speeds for the IR32-125A pump

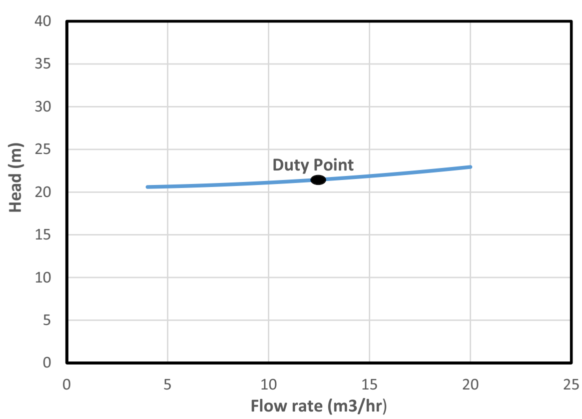

Fig. 4 Hydraulic System Load Pump

variable. The electrical motor used is SAER MT2 and its specifications are shown in Appendix 2

For any given radiation, the output power of the PV arrays represents the input power of the inverter feeding the electric motor. Since modern inverters have a high efficiency that is above 98%, if the inverter efficiency is approximated to unity, then Eq. (7) can be used to determine the actual rotation speed of the coupling shaft (motor to pump) that corresponds to the radiation value. The motor torque changes with the load change by a small amount due to the approximately flat load line and, therefore, the motor torque value in the operating region can be considered constant.

$$\omega = \frac{P_{PV} * \eta_m}{T} \tag{7}$$

where,
P_{PV} = Output of PV array.
T = Rated motor torque.

Pump operation under solar radiation

The motor is powered by electricity produced by the solar cells. This power is variable due to the change in insolation values. Therefore, the motor does not operate at its rated power through the whole daytime. The pump will operate at the operating point that results from the intersection of pump characteristic curve with the system load curve and achieve the same flow rate and head. When the power is less than the rated value, the operating point will be achieved at a rotational speed lower than the rated speed. Figure 5 shows a set of *H–Q* curves of the pump under variable speed

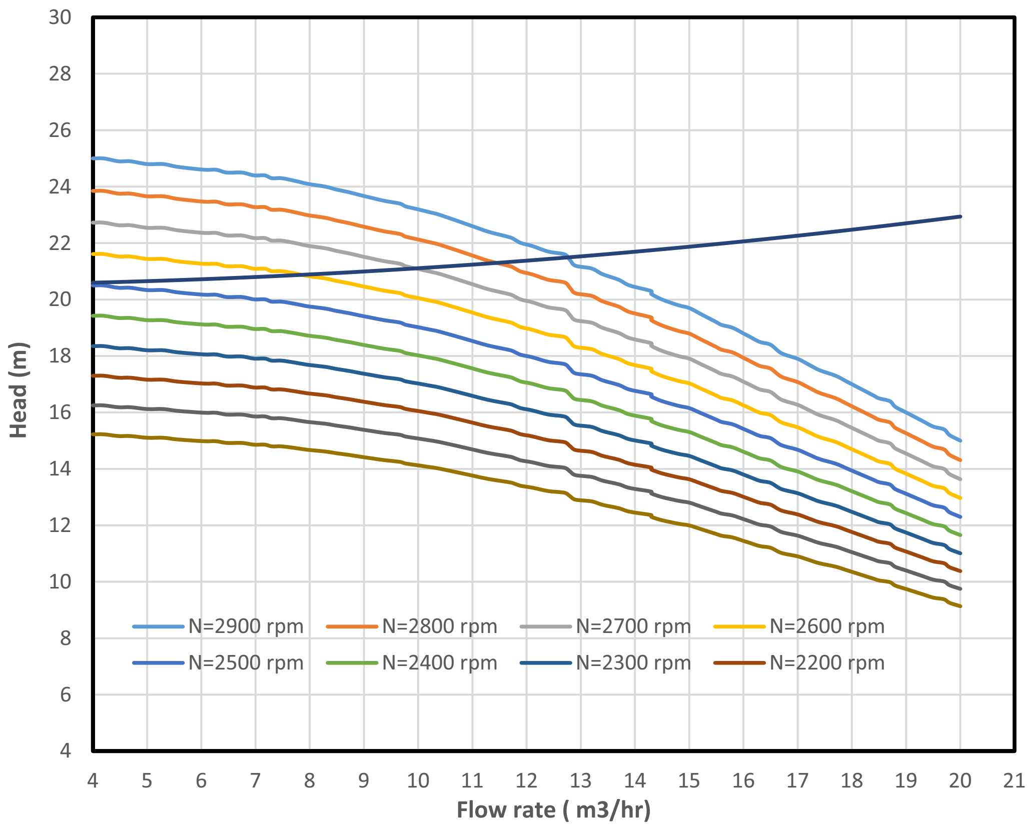

Fig. 5 A Set of *H*–*Q* curves of pump 1 at different speeds

operation and their intersection with the system curve. The upper curve is for the rated speed 2900 rpm and the lower curves are for a set of speeds that is reduced with decrementing step of 100 rpm. The operating point is determined by finding the head of the pump as a function of flow rate and solving this function with Eq. (5). Therefore, H–Q pump curves at different rotation speeds need to be found. One solution to this problem is achieved by a curve fitting program. The H–Q equation at rated speed for the specified pump is given by Eq. (8) (similar equations are determined for other speeds).

$$H = -0.0305Q^2 + 0.0909Q + 25.23 \tag{8}$$

Figure 5 shows that below a certain speed threshold, the pump H–Q characteristics will not intersect with the load hydraulic line and hence there will be no operation at these speeds. This is why a minimum speed limit is set for the inverter since below such speed no useful output is produced and the pump and motor are just heated without sufficient coolant circulation.

If N_1 is the rated speed and N_2 is the actual rotating speed of the pump. The value of N_2 depends on the input power to the electric motor. The output power of the motor which drives the pump depends on the motor efficiency. The motor efficiency changes with the load ratio and a typical motor efficiency curve as a function of the percentage of full load is given (Betka & Moussi, 2004). However, the change in motor efficiency is so small that it can be discarded. Therefore, the motor efficiency is considered constant in this work.

To determine the operating point at which the pump curve intersects the load curve, the H–Q equation of pump Eq. 8 is solved with the H–Q equation of system load (Eq. 9).

$$H = 20.5 + 0.0061Q^2 \tag{9}$$

After determining the operating point, the hydraulic power can be calculated by Eq. (10).

$$P_h = \rho \mathrm{gHQ} \tag{10}$$

We can calculate the hourly hydraulic power according to the radiation value and calculate the approximate overall day efficiency of the pump system by Eq. (11).

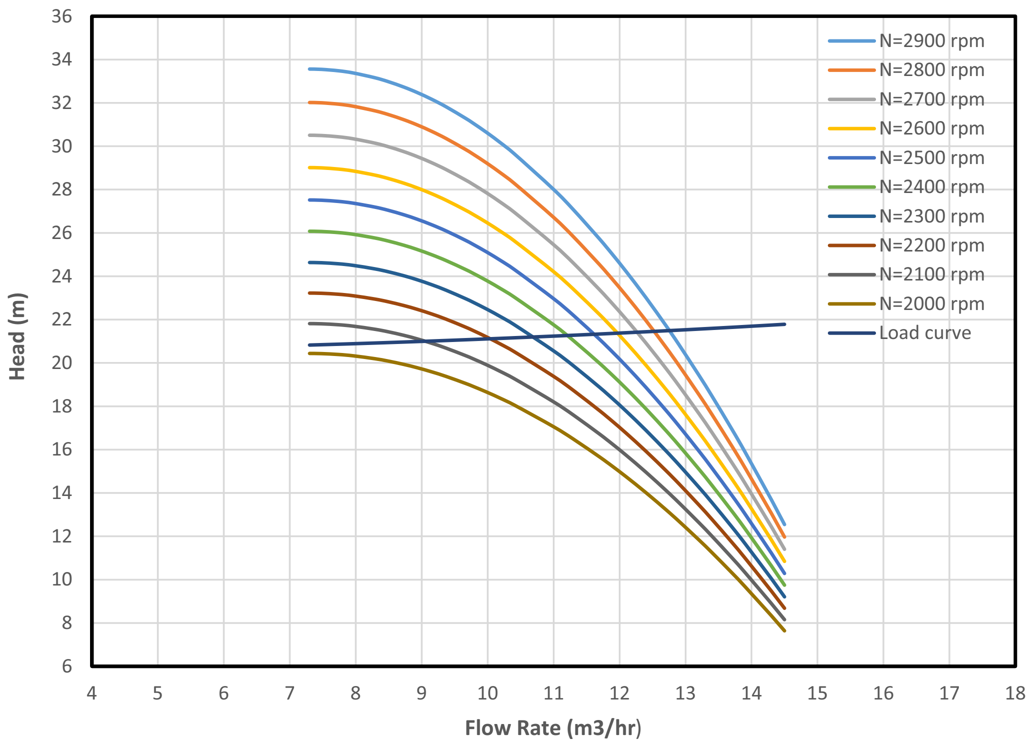

Fig. 6 A set of *H–Q* curves of pump 2 at different speeds

$$\eta_o = \frac{\rho g \sum_{i=1}^{n} H_i Q_i}{\sum_{i=1}^{n} P_{PV_i}} \quad (11)$$

where,

ρ = Water density.

g = Acceleration of gravity.

As mentioned earlier, this work compares two pumps each of them having the same peak efficiency and each of them can operate at the desired duty point with one critical difference between the two pumps. One of the two pumps has its peak efficiency occurring at the right of the duty point and the other has its peak efficiency occurring at the left of the desired duty point. Figure 5 shows the *H–Q* curves for pump 1 under different speeds with the system curve and Fig. 6 for pump 2.

Selecting the proper pump

In this work, we assume two pumps have the same maximum efficiency and the system balance is identical (PV array size, same power conditioning unit, and same electric motor). The two pumps are selected such that the duty point (H=21.5, Q=12.8) for the system load can be supplied by the two pumps as shown in Fig. 7. At this duty point the head in Eq. 6 for pump 1 is equal to the head of pump 2 which has another equation. The *H–Q* equation for pump 2 at rated speed is given by Eq. 11.

$$H = -0.405Q^2 + 5.91Q + 12 \quad (11)$$

It is obvious that the gradient of the second pump (change of H with respect to change of Q is steeper for the second pump than for the first pump). The efficiency curves for the two pumps are shown in Fig. 8. From Fig. 8, it is shown that the two pumps can be operated and provide the system with the required water. As the pump will operate at power levels lower than the rated power during a number of operating hours due to the change in radiation, the operating efficiency will change during the operating period. Therefore, the total efficiency of each pumping system will vary due to different operation points due to changing the rotational speed of the pump and working on different *H–Q* curves.

The two pumps have the same maximum efficiency but the maximum efficiency point occurs at different flow rates and different heads. For pump 1, the maximum efficiency point occurs at Q=18.7 m^3/hr and H=16.4 m while for pump 2, the maximum efficiency point occurs at Q=10.4 m^3/hr and H=23 m. As mentioned earlier, this work aims at determining the proper one of these two pumps based on the all-day efficiency.

As detailed earlier, the *H–Q* curve can be redrawn at different operating speeds according to the power values produced from the solar cells at each hour where

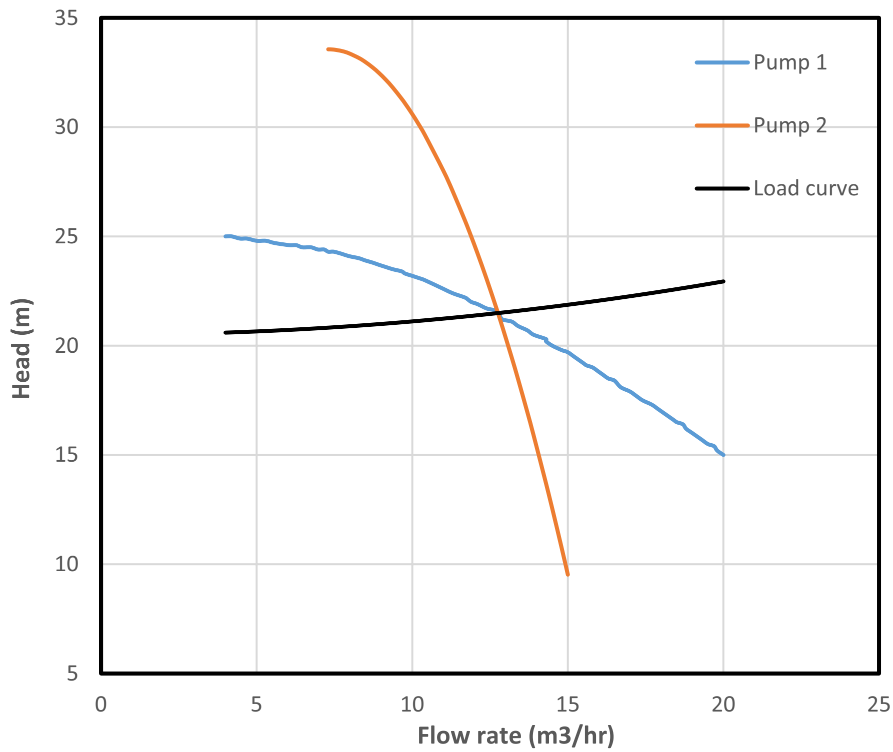

Fig. 7 The *H–Q* curves of the two pumps

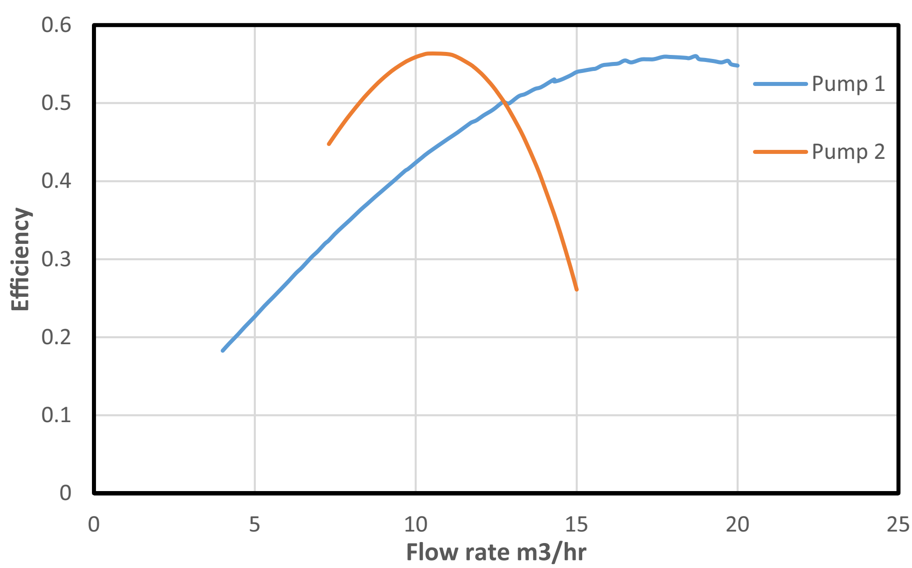

Fig. 8 The efficiency curves of the two pumps

the motor equation (Eq. No.7) is used to determine the rotational speed at each power level. Thus the operating curves of the pump at different rotational speeds can be obtained using the Eqs. (3, 4).

To determine the operating point at which each pump curve intersects with the load curve at a specific rotational speed, the *H–Q* equation of each pump at the rated speed should be adapted to the specific speed using Eq. 3. The Eq. 6 can be rewritten at the new rotational speed using the cure fitting program to obtain the H–Q equation at new speed. Then we get the operating point by equalization the head equation of the pump by the head equation of the load system.

Results and discussions

Operating at duty point

The performance of the pump should be evaluated throughout the year. However, to simplify the analysis, the performance was evaluated during a day of low radiation equal to 3 kW/m^2/day and another day of high radiation equal to 7.3 kW/m^2/day. Figure 7 shows that pump 1 does not operate with the system load if the speed is less than 2500 rpm. Figure 8 shows that pump 2 is operating at a wide range of speeds compared with pump 1. Therefore, at the low radiation days, the number of operating hours for pump 2 is more than the number of operating hours for pump 1.

The operating efficiency along time slots of one hour of each pump is shown in Table 1 for a low radiation day and another high radiation day. From the results, it is shown that the operating efficiency of pump 2 is higher than that of pump 1.

The efficiency of the two pumps is identical at rated speed but the efficiency of pump 2 is higher than pump 1 at all speeds less than the rated speed. From Fig. 5 it is shown that pump 1 is not operable at a speed less than 2500 rpm. This means that the minimum electrical power required to operate the pump with the load is 1280 W which corresponds to the value of radiation equal to 0.713 kW/m^2. On the other hand, pump 2 can be operated at speeds down to 2100 rpm. This means that the minimum electrical power required to operate the pump with the load is 1080 W which corresponds to the value of radiation equal to 0.6 kW/m^2. Therefore, pump 2 is not only more efficient but also gives more water. To compare two pumps operating at the same operating point, the H–Q curve for each of them will differ in slope. It is shown from the results that the pump with a higher slope is higher in all-day efficiency as well.

Operating at constant head

In most applications, the pump is installed in a stationary system to raise the required amount of water. For the comparison to be complete, the performance of each pump at a constant head should be studied. The performance of each pump was studied at a head above the operating point (22 m) and another below the operating point (15 m).

Operating at head 22 m

Figures 5, 6 show that pump 1 can operate with a 22 m head at a speed of more than 2750 rpm while pump 2 may operate at a speed slightly more than 2250 rpm with the same head. The operation results for two pumps at low and high radiation days are illustrated in Table 2.

Graphically, pump 2 which has a high slope will give a higher flow rate. So, the efficiency and total performance of pump 2 is better than pump 1.

From the results shown in the table, we find that at low rates of radiation, pump 1 does not operate at low radiation and doesn't give water. For a head equal to 15 m, Pump 2 is better than Pump 1.

Operating at head 15 m

In the case of installing the pumps to raise the water to a fixed height lower than the proposed duty point, the performance evaluation is different. Pump 1 has a low slope will give a higher flow rate. This result is shown in Table 3.

From the results shown in the table, we find that at low rates of radiation, pump 1 is better than pump 2, but it may not give the required amount of water due to the small number of operating hours.

Table 1 Operating the two pumps at duty point

Operating hour	Low radiation day efficiency %			High radiation day efficiency %		
	Operating speed (rpm)	Pump 1	Pump 2	Operating speed (rpm)	Pump 1	Pump 2
1	2330	Not operating	42	2550	15	41
2	2530	16	42.3	2820	37	40.8
3	2650	29	43	2900	38	38
4	2350	Not operating	42.5	2900	39.6	39.6
5				2830	37	40.5
6				2600	27	42
Day eff.		22.6	42.5		32.8	40.3

Table 2 Operating the two pumps at constant head 22 m

Operating hours	Low radiation day flow rate (Q) m^3/hr			High radiation day flow rate (Q) m^3/hr		
	Operating speed (rpm)	Pump 1	Pump 2	Operating speed (rpm)	Pump 1	Pump 2
1	2330	Not operating	10.3	2550	Not operating	11.3
2	2530	Not operating	11.3	2820	10.4	12.5
3	2650	Not operating	11.9	2900	11.9	12.6
4	2350	Not operating	10.4	2900	11.9	12.6
5				2830	10.4	12.5
6				2600	Not operating	11.8

Table 3 Operating the two pumps at constant head 15 m

Operating hours	Low radiation day flow rate (Q) m^3/hr			High radiation day flow rate (Q) m^3/hr		
	Operating speed (rpm)	Pump 1	Pump 2	Operating speed (rpm)	Pump 1	Pump 2
1	2330	Not operating	13	2550	16.5	13.5
2	2530	16.5	13.5	2820	19.2	13.8
3	2650	17.6	13.8	2900	20	14.1
4	2350	Not operating	13	2900	20	14.1
5				2830	19.2	13.8
6				2600	17.5	13.7

Selecting the proper pump

The method proposed in this work can be used to select the pump that best fits the requirements of a given photovoltaic pumping system. The traditional method for pump selection is applied to obtain the maximum efficiency with the load requirements. When the pump system is supplied electrically from solar cells, it's found that the rotational speed of the pump is varied because the electrical power is changed with radiation values. The location of the maximum efficiency point on the H–Q curve of each pump depends on some impeller design parameters. From the results of the comparison, it is shown that the efficiency of each pump at each operating hour is different. So, the overall day efficiency is different for the two pumps. In general, pump #2 which has a steeper H–Q curve gives higher all-day efficiency. In the case of operating at the desired load (H, Q) point, the efficiency of pump 1 is 22.6% and pump 2 is 42.5% for low radiation day. At high radiation days, the overall efficiency and water quantity are increased for two pumps. The efficiency of pump 1 is 32.8% and pump 2 is 40.3%. If the pumps are operating at a constant head higher than the pre-designated head, pump 2 is the best compared with pump 1. The results at a constant head equal to 22 m showed that pump 1 is not operable at low radiation because the low power results in low speed and pump 1 can't operate under 2500 rpm with a head of 22 m.

At a head lower than the pre-designated head, the pump with a lower inclination curve gives higher efficiency. Therefore, pump 1 in this case gives high all-day efficiency compared with pump 2.

Conclusion

In this paper, a comparative study is presented to choose the most suitable pump to work with the solar cell system. Two pumps with different characteristics are compared at the same operating point with the required load system. The characteristic curve of each pump is different in inclination, but they have a common operating point and the same maximum efficiency value. The rotation speed of the pump changes with the change in the value of the power produced by the solar cell system. The performance of each pump has been studied at different levels of radiation and different rotational speeds. When choosing the best pump to operate at a specific duty point, the duty point should be located to the right of the pump's maximum efficiency point. If for some reason, the load requirements increase in the head for the same setup, the pump that has a steeper characteristic curve will outperform the one with a lower slope with respect to the all-day efficiency. Conversely, if the load head requirements are decreased for the same setup, the pump with a lower slope of the characteristic curve is preferable. In the future, a software program can be prepared to choose the best pump that gives the highest operating efficiency with changing solar radiation values.

Appendix 1

Model No	OPS-100M
Maximum Power (P_{max})	100 W_P
Voltage at Maximum Power (V_{mpp})	19.8 V
Current at Maximum Power (I_{mpp})	5.05 A
Open Circuit Voltage (V_{oc})	22.6 V
Short Circuit Current (I_{sc})	5.45 A
Module Efficiency	20%
Module Dimensions (*H/W/D*)	1020 × 510 × 30 mm
Cell Type	Monocrystalline

Appendix 2

Model No	SAER MT2-IE2-80-2P-2
Nominal power	1.5 kW
Voltage	400 V
Current	3.3 A
Motor efficiency	82%
Number of poles	2
Rated speed	2900 rpm
Starting mode	Star/delta
Frequency	50 Hz

Abbreviations

BEP Best Efficiency Point
MPPT Maximum Power Point Tracking
PR Performance ratio
PV Photovoltaic
PVPS Photovoltaic Pumping System

List of symbols

A Solar array area
g Acceleration of gravity
H Total head
h Static head
K Friction factor
N Rotational speed
P Power
Q Water Flow rate
T Rated motor torque
$\varnothing$ Maximum solar radiation
ω Angular speed
ρ Water density
η Efficiency

Subscripts

h Hydraulic
m Motor
c Control unit
o Overall day

Acknowledgements
The authors thank the Electronics Research Institute.

Author contributions
The first author (Corresponding author) designed the system, performed the simulation, analysed the results and writing the article. The second author suggested the method, presented literature review, analysis of results, and review writing.

Funding
The research was done in my institute "Electronics Research Institute".

Availability of data materials
All data are available in the article, except for solar radiation values, which can be obtained from any atlas of the geographical area.

Declarations

Ethics approval and consent to participate
Not applicable.

Consent for publication
Not applicable.

Competing interests
The authors declare that have no competing interests.

Received: 29 March 2023 Accepted: 30 November 2023
Published online: 21 December 2023

References

Abdelmalek, M., Abdelhamid Midoun, D., Kadri, S. H., & Raja, I. A. (2011). 'Performance of a directly-coupled PV water pumping system. *Energy Conversion and Management', 52*(10), 3089–3095.
Abdourraziq, S., & El Bachtiri, R. (2017). A comparative study between photovoltaic pumping systems using a permanent magnet DC motor and an induction motor. In A. Sayigh (Ed.), *Mediterranean Green Buildings & Renewable Energy*. Springer, Cham.
Ahonen, T., Tamminen, J., Ahola, J., & Kestila, J. (2012). Frequency-converter-based hybrid estimation method for the centrifugal pump operational state. *IEEE Transactions on Industrial Electronics, 59*(12), 4803–4809.
Allouhi, A., Buker, M. S., El-houari, H., Boharb, A., Benzakour Amine, M., Kousksou, T., & Jamil, A. (2019). PV water pumping systems for domestic uses in remote areas: sizing process, simulation and economic evaluation. *Renewable Energy, 132*, 798–812.
Almeida, R., Ledesma, J., Carrˆelo, I., Narvarte, L., Ferrara, G., & Antipodi, L. (2018). A new pump selection method for large-power PV irrigation systems at a variable frequency. *Energy Conversion and Management, 174*, 874–885.
Alonso-Abella, M., Lorenzo, E., & Chenlo, F. (2003). PV water pumping systems based on standard frequency converters. *Progress in Photovoltaics: Research and Applications, Vo., 11*(3), 179–191.
Babkir, A. (2018). Comparative assessment of the feasibility for solar irrigation pumps in Sudan. *Renewable and Sustainable Energy Reviews., 81*, 413–420.
Bansal, R. K. (2010). A Text Book of Fluid Mechanics and Hydraulic Machines. LAXMI Publication (P) LTD, New Delhi-110002.
Belkacem, B. (2013). New sizing method of PV water pumping systems. *Sustainable Energy Technologies and Assessments, 4*, 1–10.

Betka, A., & Moussi, A. (2004). Performance optimization of a photovoltaic induction motor pumping system. *Renewable Energy, 29*(14), 2167–2181.
Boutelhig, A., Hadjarab, A., & Bakelli, Y. (2011). Comparison study to select an optimum photovoltaic pumping system (PVPS) Configuration upon experimental performances data of two different DC pumps tested at ghardaïa site. *Energy Procedia, 6*, 769–776.
Chandel, S. S., NagarajuNaik a, M., & Chandelb, R. (2015). Review of solar photovoltaic water pumping system technology for irrigation and community drinking water supplies. *Renewable and Sustainable Energy Reviews, 49*, 1084–1099.
Chandrasekaran, N., & GaneshprabuThyagarajah, B. N. (2012). MATLAB based comparative study of photovoltaic fed DC motor and PMDC motor pumping system. *ARPN Journal of Engineering and Applied Sciences, 7*(5), 543–547.
dos Wanderlley Sena, S., Torres, P. F., Brito, A. U., Manito, A. R., Pinto Filho, G. F., Monteiro, W. L., & Macedo, W. N. (2021). A novel method to determine the optimal operating point for centrifugal pumps applied in photovoltaic pumping systems. *Solar Energy, 221*, 46–59.
Gasque, M., Gonz´alez-Altozano, P., Guti´errez-Colomer, R. P., & García-Marí, E. (2020). Optimisation of the distribution of power from a photovoltaic generator between two pumps working in parallel'. *Solar Energy, 98*, 324–334.
Gasque, M., Gonz´alez-Altozano, P., Guti´errez-Colomer, R. P., & García-Marí, E. (2021). Comparative evaluation of two photovoltaic multi-pump parallel system configurations for optimal distribution of the generated power. *Sustainable Energy Technologies and Assessments, 48*, 1–11.
Ghoneim, A. A. (2006). Design optimization of photovoltaic powered water pumping systems. *Energy Conversion and Management, 47*, 1449–1463.
Gutierrez, J., Merino, G., Lara, D., & Salazar, L. (2021). Hydraulic assessment of a photovoltaic system driving a conventional AC surface electric pump. *Sustainable Energy Technologies and Assessments, 45*, 1–11.
Kolhe, M., Joshi, J. C., & Kothari, D. P. (2004). Performance analysis of a directly coupled photovoltaic water-pumping system. *IEEE Transaction on Energy Conversion, 19*(3), 613–618.
Koor, M., Vassiljev, A., & Koppel, T. (2016). Optimization of pump efficiencies with different pumps characteristics working in parallel mode. *Advances in Engineering Software, 101*, 69–76.
Odeh, I. (2013). Introducing new design and performance points for photovoltaic water pumping systems based on long-term field data analysis. *Journal of Renewable and Sustainable Energy, 5*(2), 023135.
Rahrah, K., Rekioua, D., Rekioua, T., & Bacha, S. (2015). Photovoltaic pumping system in Bejaia climate with battery storage. *International Journal of Hydrogen Energy, 40*(39), 13665–13675.
Renu, B. B., Prasad, B., Sastry, O. S., Kumar, A., & Bangar, M. (2017). Optimum sizing and performance modeling of Solar Photovoltaic (SPV) water pumps for different climatic conditions. *Solar Energy, 155*, 1326–1338.
Roberto Valer, L., Melendez, T. A., Cristina Fedrizzi, M., Zilles, R., & de Moraes, A. M. (2016). Variable-speed drives in photovoltaic pumping systems for irrigation in Brazil. *Sustainable Energy Technologies and Assessments, 15*, 20–26.
SAER ELECTROPOMPE Company (2019) SAER Pump Selector Software.
Xie, H., Ringler, C., & Mondal, M. A. (2021). Solar or diesel: a comparison of costs for groundwater- fed irrigation in sub-saharan africa under two energy solutions. *Earth's Future Journal, 9*, 1–21.
Yadav, K., Kumar, A., Sastry, O. S., & Wandhare, R. (2019). Solar photovoltaics pumps operating head selection for the optimum efficiency. *Renewable Energy, 134*, 169–177.

Publisher's Note